

Tuning supramolecular G-quadruplexes with mono- and divalent cations

Mariana Martín-Hidalgo, Marilyn García-Arriaga, Fernando González and José M. Rivera*

Department of Chemistry, University of Puerto Rico, Río Piedras Campus, Río Piedras 00931, Puerto Rico

(Received 4 April 2014; accepted 9 May 2014)

Supramolecular G-quadruplexes (SGQs) are formed via the cation promoted self-assembly of guanine derivatives into stacks of planar hydrogen-bonded tetramers. Here, we present results on the formation of SGQs made from the 8-(*m*-acetylphenyl)-2'-deoxyguanosine (**mAGi**) derivative in the presence of various mono- and divalent cations. NMR and HR ESI-MS data indicate that varying the cation can efficiently tune the molecularity, the fidelity and stability (thermal and kinetic) of the resulting SGQs. The results show that, parallel to the previously reported potassium-templated hexadecamer (**mAGi**₆·3K⁺), Na⁺, Rb⁺ and NH₄⁺ also promote the formation of similar supramolecules with high fidelity and molecularity. In contrast, the divalent cations Pb²⁺, Sr²⁺ and Ba²⁺ template the formation of octamers (**mAGi**₈), with the latter two inducing higher thermal stabilities. Molecular dynamics simulations for the hexadecamers containing monovalent cations enabled critical insights that help explain the experimental observations.

Keywords: self-assembly; cation recognition; G-quadruplex

Introduction

Guanosine is a privileged recognition motif for the development of discrete supramolecular self-assembled nanostructures (1). It is known that guanosine, deoxyguanosine and related derivatives can form hydrogen-bonded tetrameric structures (a.k.a. G-tetrads and G-quartets) that coaxially stack upon the addition of a wide variety of cations, to form supramolecular G-quadruplexes (SGQs) (Figure 1(a)) (2). G-rich oligonucleotides (e.g. DNA and RNA) can also self-assemble and/or fold into G-quadruplexes, which we term here oligo-GQs or OGQs. Both the structure and stability of SGQs can be modulated by either covalent modifications of the assembling subunits (intrinsic parameters) (3) or by changes of extrinsic parameters such as the cation/anion (4) and the solvent (5). For example, we have previously reported that modifications at the C8 of the guanine moiety with aryl or hetero aryl groups (8ArG) enable the reliable formation of precise supramolecules (i.e. discrete and of well-defined size and composition) (3). The 8-(*m*-acetylphenyl)-2'-deoxyguanosine moiety has been of special interest because its reliable potassium cation promoted self-assembly into hexadecameric supramolecules; this happens in both organic (3a) and aqueous media (6), and even after covalently attaching bulky groups such as dendrons (3). We have also shown that the hexadecamer formed by the lipophilic derivative 8-(*m*-acetylphenyl)-2'-deoxyguanosine (**mAGi**) (Figure 1(a)) in acetonitrile, replacing the cation from potassium to strontium, enabled the reversible high fidelity switching to the corresponding octamer (7).

Such results prompted us to perform a systematic study to determine the effect of other mono- and divalent cations on the self-assembly of the same 8ArG derivative.

The wide interest in elucidating the role of the cation (8) in the structure and dynamics of SGQs is evident by the multiple studies addressing, for example, the effect on molecularity (amount of subunits), fidelity (9) (per cent of desired structures) and stability (thermodynamic and kinetic) of such structures, when in the presence of monovalent (10), divalent (11) and even trivalent (12) metal cations (2). This interest has also been fuelled by the potential use of SGQs as self-assembled ionophores due to their varied cation affinities and selectivities (13).

Here, we report the results of NMR, ESI-MS and molecular dynamics simulations (MDS) on the self-assembly of **mAGi** in the presence of monovalent cations such as Li⁺, Na⁺, K⁺, Rb⁺, Cs⁺, Tl⁺ and NH₄⁺ and of divalent cations such as Sr²⁺, Ba²⁺ and Pb²⁺ (Figure 1(c)). Our results indicate that cation properties such as charge, size and electron density dictate the molecularity, fidelity and stability (thermal and kinetic) of the resulting SGQs. We expect this information to be useful in the further development of SGQs for the construction of functional supramolecular systems.

Results and discussion

Monovalent cations

The ¹H NMR spectra of **mAGi** (30 mM in CD₃CN) with different iodide salts were used to evaluate the

*Corresponding author. Email: rivalab.upr@gmail.com

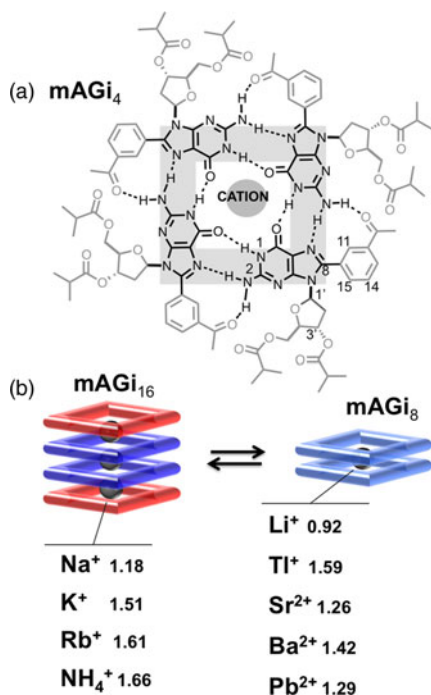


Figure 1. (Colour online) (a) Kekulé representation for the tetramer (a.k.a. tetrad) formed by the 8ArG derivative **mAGi** with the parent G-tetrad highlighted in grey. (b) Cartoon representation of two possible SGQs formed by **mAGi**: the hexadecamer (**mAGi₁₆**) and the octamer (**mAGi₈**). The outer and inner tetrads for **mAGi₁₆** are coloured red and blue, respectively, while the octamer is coloured light blue. The same colouring scheme is used in Figures 2 and 7. The values for effective ionic radii correspond to octahedrally coordinated cations used in this study. The cations are grouped on the left and right for those that promote the formation of hexadecamers and octamers, respectively.

supramolecular assemblies promoted by each of the aforementioned cations. The resulting spectra, after addition of NaI, RbI or NH₄I (0.5 equiv.), showed very similar signals to the previously reported potassium-promoted hexadecamer **mAGi₁₆** (Figure 2(c)–(f)) (3a), including a series of characteristic cross-peak patterns in the 2D NOESY spectra (Figure 3). HR-ESI MS experiments show clean spectra with prominent peaks matching the masses for [**mAGi₁₆**·3Na]³⁺ (*m/z* 2825.8347), [**mAGi₁₆**·3NH₄]³⁺ (*m/z* 2820.7881) and [**mAGi₁₆**·3Rb]³⁺ (*m/z* 2888.3225), although the latter with a lower relative abundance (Figure 3). As stated earlier, the NMR spectra show that Na⁺, Rb⁺ and NH₄⁺ promote the formation of a very similar hexadecamer to the one promoted by K⁺, nevertheless, there are some subtle differences (6). Specifically, the chemical shifts for the N1H signals for the outer (red) and inner (navy blue) tetrads of **mAGi₁₆** are affected to a greater extent. While the signal corresponding to the inner tetrad of **mAGi₁₆** remains reasonably constant at around 11.2 ppm (Figure 2(c)–(f), navy blue signal), the signal corresponding to the

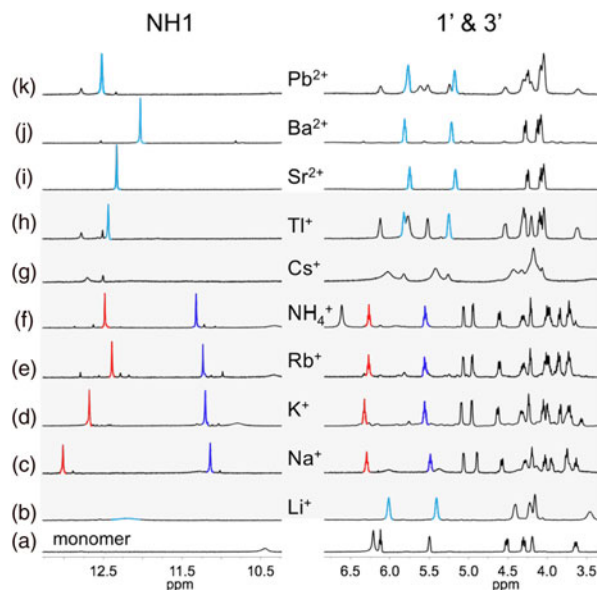


Figure 2. (Colour online) Partial ¹H NMR spectra (500 MHz, 298.2 K) showing the region for the peaks corresponding to N1H, H1' and H3' for **mAGi** (30 mM) with: (a) no salt; (b) LiI, 95% **mAGi₈**·Li⁺; (c) NaI, 95% **mAGi₁₆**·3Na⁺; (d) KI, 90% **mAGi₁₆**·3K⁺; (e) RbI, 67% **mAGi₁₆**·3Rb⁺; (f) NH₄I, 86% **mAGi₁₆**·3NH₄⁺; (g) CsI, unidentified species; (h) TlI, 58% **mAGi₈**·Tl⁺; (i) SrI₂, ~100% **mAGi₈**·Sr²⁺; (j) BaI₂, 90% **mAGi₈**·Ba²⁺; and (k) PbI₂, 77% **mAGi₈**·Pb²⁺. The spectra highlighted in light grey correspond to the samples containing monovalent cation salts. All the samples contain 0.5 equiv. of the iodide salts with the exception of SrI₂ and BaI₂ (0.125 equiv.). Selected peaks from **mAGi₈** are coloured in light blue while the outer and inner tetrads in **mAGi₁₆** are coloured red and blue, respectively.

outer tetrad (Figure 2(c)–(f), red signal) shows a downfield shift as the ionic radius of the cations increases. Smaller ions like Na⁺ strongly polarise the carbonyls of the outer tetrads, which in turn induces a deshielding of the N1H protons when compared with bigger cations like NH₄⁺ (Figure 2(f)). In contrast, the region corresponding to the H1'/3' reveals fairly constant chemical shifts due to their relatively further distance from the cation coordination site. Although Rb⁺ (1.61 Å) is not significantly larger than K⁺, and similar in size to NH₄⁺, we hypothesise that the lower fidelity (e.g. small amounts of unidentified assemblies in the NMR) and stability of **mAGi₁₆**·3Rb⁺ result from inter-cationic repulsion due to its higher relative electron density.

Moving from K⁺ to smaller (e.g. Li⁺; 0.92 Å) (14) or larger cations (e.g. Cs⁺; 1.74 Å) (15) is detrimental to the formation of SGQs (Figure 2). Addition of lithium iodide (0.5 equiv.) to a solution of **mAGi** leads to a ¹H NMR spectrum with broader peaks (Figure 2(b)) relative to the one recorded prior to adding the salt (Figure 1(a)). The peaks corresponding to H1' and H3' are shifted upfield, while the N1H peak (~12 ppm) is broadened to the point

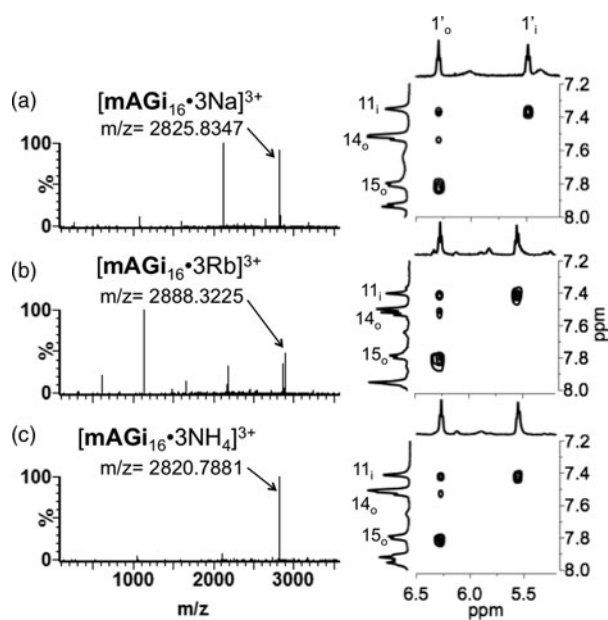


Figure 3. HR-ESI MS for the hexadecamer **mAGi**₁₆ promoted by (a) Na⁺, (b) Rb⁺, (c) NH₄⁺ (left) and selected partial 2D NOESY spectra (500 MHz, 298.2 K, CD₃CN) showing key signature cross-peaks (6). The corresponding complete spectra are shown in Figures S11–S13.

of being almost undetectable, suggesting a more dynamic system (i.e. faster exchange of the **mAGi** subunits). HR-ESI-MS experiments reveal a prominent base peak for $[\text{mAGi}_8 \cdot 2\text{Li}]^{2+}$ (m/z 2109.1572), which support the formation of a dynamic octamer (**mAGi**₈) in solution. This behaviour is presumably a consequence of the greater desolvation energy of Li⁺ ions combined with its preferential binding coplanar to the tetrad. The latter precludes the simultaneous coordination of the O6 of two consecutive tetrads making their coaxial stacking more difficult. At the other end of the size range, experiments with Cs⁺ reveal it to also be unsuitable at promoting the formation of SGQs (Figure 1(g)). This phenomenon, however, might be limited to SGQs formed by **mAGi** and other 8ArG derivatives since Davis et al. (16) have reported the formation of SGQs promoted by Cs⁺ ions.

Based on its size (1.59 Å) (14), and the fact that it is monovalent, Tl⁺ should promote the formation of a hexadecamer. Thallium has proven useful in structural studies of OGQs by X-ray crystallography due to its high electron density (17). Our results show that, while Tl⁺ does in fact promote the assembly of **mAGi** (Figure 1(h)) with modest fidelity (58%), instead of the anticipated hexadecamer, the resulting SGQ is an octamer (**mAGi**₈-Tl⁺) of low relative stability ($T_m = 304$ K; Figure 5). We hypothesise that this results from the relatively low solubility of TII in acetonitrile (as indicated by the fact that some of the salt precipitated during sample preparation). This parallels our previous report on the shift in the

equilibrium from a hexadecamer to an octamer by a derivative closely related to **mAGi**, in which the availability (i.e. activity) of the promoting K⁺ ions was modulated by the polarity of the solvent used (acetonitrile vs chloroform) (5a).

Divalent metal cations

We have previously reported a metallo-responsive SGQ that switched, respectively, between hexadecameric and octameric states when the metal cation was changed from potassium to strontium. Intrigued by these results, we tested the effects of other divalent cations, specifically Ba²⁺ and Pb²⁺. NMR studies reveal that, similar to strontium, such cations promote the preferential formation of octamers, although with slightly lower fidelities (Figure 1(i)–(k)) and thermal stabilities ($T_m = \text{Sr}^{2+} \sim \text{Ba}^{2+} > \text{Pb}^{2+}$). The corresponding HR-ESI MS spectra (Figure 4) show good correlation with the NMR experiments, similar to the corresponding experiments with monovalent cations.

Parallel to Tl⁺, the divalent metal cations Sr²⁺, Ba²⁺ and Pb²⁺ promote the formation of the octamer **mAGi**₈, although with higher fidelity and thermal stability (Figure 4). Formation of a hexadecamer would require three consecutive divalent cations between the four tetrads leading to enhanced charge–charge repulsion that would shift the equilibrium towards the corresponding octamer. This behaviour is consistent to the one reported by the Wu group (11b) in which the lipophilic 2',3',5'-O-triacetyl-

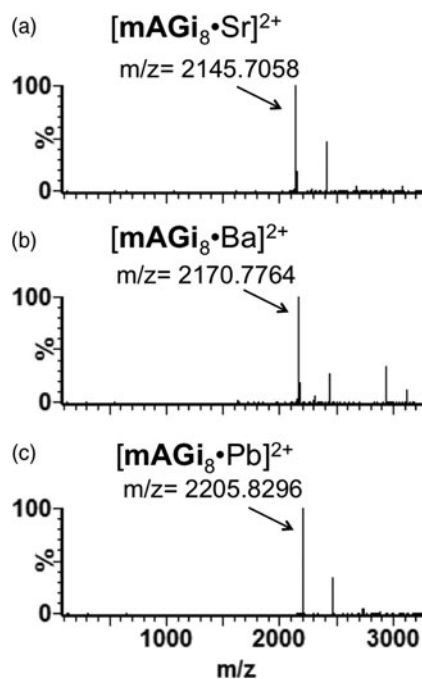


Figure 4. HR-ESI-MS for the octamers (**mAGi**₈) promoted by (a) Sr²⁺, (b) Ba²⁺ and (c) Pb²⁺.

guanosine derivative formed octamers in the presence of Ca^{2+} , Sr^{2+} and Ba^{2+} . In contrast, Davis reported the formation of hexadecameric SGQs by lipophilic guanosine derivatives induced by strontium, barium (4b, 4c) and lead (11a) cations. These hexadecamers, however, were in essence dimers of octamers in which a belt of four picrate anions interacted strongly (via attractive charge–charge interactions and the formation of H-bonds) with the guanosine subunits of the two inner G-tetrads.

Thermal stability studies

Variable temperature ^1H NMR experiments (Figures 5, S20–S32) reveal that the hexadecamer templated by K^+ (1.51 Å) (14) ($\text{mAGi}_{16}\cdot 3\text{K}^+$) is about 20 K more thermally stable than those templated by Na^+ (1.18 Å) and NH_4^+ (1.61 Å) (15). The resulting trend in thermal stability ($\text{K}^+ > \text{NH}_4^+ \sim \text{Na}^+ \gg \text{Rb}^+$) is consistent to the one reported with other SGQs and OGQs (18). Divalent cations reveal mixed results, with the octamers (mAGi_8) templated by Sr^{2+} and Ba^{2+} showing enhanced stability relative to $\text{mAGi}_{16}\cdot 3\text{K}^+$ ($\Delta T_m > +5$ K) while Pb^{2+} resulted in an octamer with lower stability ($\Delta T_m = -16$ K) closer to those of the hexadecamers templated by Na^+ and NH_4^+ . The enhanced stability induced by Sr^{2+} and Ba^{2+} is consistent with reports with both OGQs and SGQs where the enhancement has been attributed to a stronger coordination between O6 of the guanine moieties (18b).

Lead(II) ions have also been reported to be effective promoters for the formation of OGQs (19) and SGQs (11a, 19d), and this characteristic has been exploited in the development of OGQ-based sensors (20). The 8-aryl-substituted mAGi derivative, however, forms a hexadecamer of lower stability in contrast to the report by Davis (11a) indicating the formation of a lead(II)-templated hexadecamer of enhanced kinetic stability. We hypothesise this phenomenon results from a decreased activity of lead cations from PbI_2 in acetonitrile (relative to the lead picrate used by

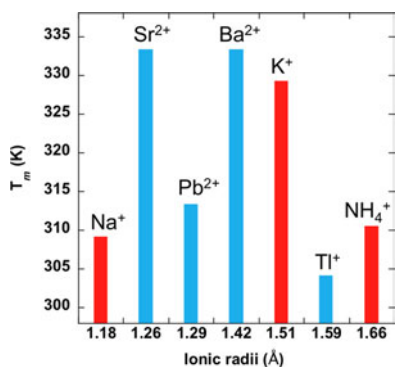


Figure 5. (Colour online) Melting temperatures (T_m) for various SGQs (octamer, red; hexadecamer; light blue) formed by mAGi (5 mM) as promoted by various cations. All the T_m values were determined by ^1H NMR and have an estimated 5% error.

Davis), which is parallel to the aforementioned results with TII.

MDS studies

Atomistic MDS studies provided additional information that complement the NMR and MS experiments (15). MDS studies have provided critical insights into the effects of changes in the sequence, cations and binding of small molecules on the structure and dynamics of OGQs (15, 21). Specifically, detailed assessments of the dynamics of cations moving in and out of the central channel of OGQs were recently reported by Reshetnikov et al. (22) and Akhshi et al. (23) using, respectively, the thrombin-binding aptamer and a tetramolecular OGQ.

We carried out MDS with $\text{mAGi}_{16}\cdot 3\text{X}^+$ and $\text{mAGi}_8\cdot \text{X}^+$ where X^+ represents the aforementioned monovalent cations (with the exception of TI^+). The starting structures were constructed by replacing the potassium cations in $\text{mAGi}_{16}\cdot 3\text{K}^+$ and $\text{mAGi}_8\cdot \text{K}^+$ with the corresponding cation of interest.¹ The stability of the SGQs was assessed taking into consideration a combination of the following criteria: (1) changes in the RMSD values as a function of time (Figure 6(a)); (2) the probability density as a function of RMSD (Figure 6(b)) and (3) a visual inspection of structures at the end of the simulation (Figure 7). For the first criterion, large deviations in RMSD values relative to

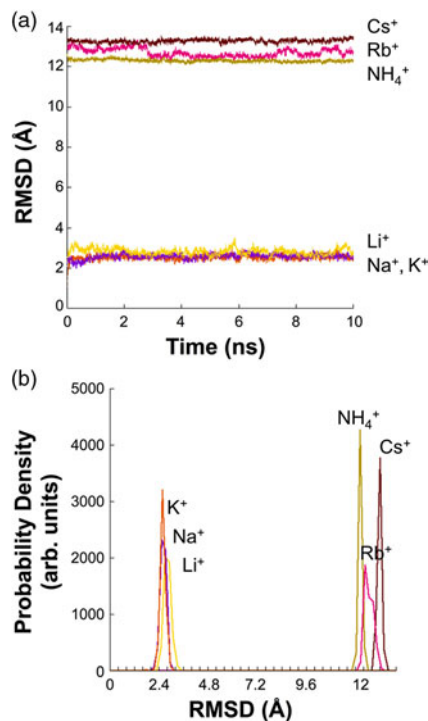


Figure 6. (Colour online) (a) Trajectory of the dynamics and (b) distribution of the RMSD for mAGi_{16} with Li^+ (blue), Na^+ (purple), K^+ (orange), Rb^+ (pink), NH_4^+ (gold) and Cs^+ (burgundy red).

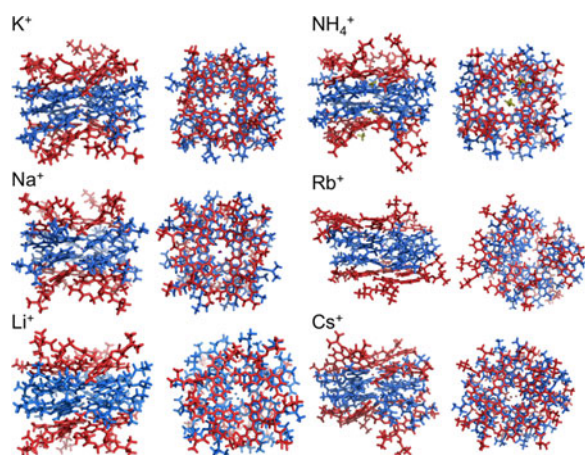


Figure 7. (Colour online) Final structures for the hexadecamers ($\mathbf{mAGi}_{16}\cdot 3X^+$) formed with the indicated monovalent cations. For each cation, the resulting structures are shown in side (first and third columns) and top (second and fourth columns) views, respectively. Similar to in Figure 1, the outer and inner tetrads are coloured red and blue, respectively.

an idealised $\mathbf{mAGi}_{16}\cdot 3K^+$ or $\mathbf{mAGi}_8\cdot K^+$ structure (based on 1D/2D NMR studies) (6) were taken as an indication of relative instability, as were systems with a positive slope in the trajectory. For the second criterion, sharper (i.e. narrower and higher) peaks reflect a lower spread of the distributions, and SGQs that have reached a relatively stable configuration. The third criterion is especially important in cases in which, despite the first two criteria suggesting a putative stable structure (e.g. flat RMSD trajectory and a narrow RMSD distribution), but where the supramolecular arrangement of subunits deviate significantly from the idealised features of SGQs (e.g. planar co-axial tetrads, presence of internal cations and appropriate *syn/anti* conformation of the G-subunits).

In general, and in all the simulated hexadecamers ($\mathbf{mAGi}_{16}\cdot 3X^+$), the individual constituent subunits showed negligible changes in the sugar pucker (of the 2'-deoxyguanosine moieties) and relatively small changes in the glycosidic angles (Figure 7). Throughout the entire simulation, the central channel maintains an average diameter of 2.5 Å, but fluctuations of up to 5.2 Å (in the outer tetrads) enable the free movement of cations. The intra-tetrad hydrogen-bond patterns are largely conserved despite deviations from planarity, with the largest deviations found for the Rb^+ - and Cs^+ -containing hexadecamers. For all the systems, the outer tetrads (highlighted in red in Figure 7) showed the greatest deviations from planarity as expected due to the greater freedom for the constituent subunits.

Analysis of the RMSD trajectory for the average structures of \mathbf{mAGi}_{16} with the smaller cations (Li^+ , Na^+ and K^+) reveals a low average RMSD value with a narrow

structural distribution peak at around 2.4 Å (Figure 6). Although $\mathbf{mAGi}_{16}\cdot 3Li^+$ is not observed experimentally, we can deduce from these studies that a putative hexadecamer containing Li^+ would be akin to $\mathbf{mAGi}_{16}\cdot 3Na^+$ due to their similar RMSD values and probability densities (Figure 6 (b)). Simulations of $\mathbf{mAGi}_8\cdot Li^+$ are consistent with the experimental observation of an unstable octamer with an average RMSD of 5 Å and a broader structural distribution than the one observed for $\mathbf{mAGi}_8\cdot K^+$ (Figures S35–S37). Bowman et al. (24) have used the terminologies condensed, glassy and coordinated to label the level of affinity (lowest to highest, respectively) of different cations towards specific nucleic acid structures (including OGQs). These classifications take into consideration multiple parameters such as their contributions to the kinetic and thermodynamic stability of the specific structure, diffusion characteristics and the extent of ion coordination. While the alkali cations Na^+ , K^+ and Rb^+ should be considered as the coordinated type, Li^+ can be classified as a glassy cation, because the evidence is consistent with its interaction with the SGQs, but its small size preclude a stronger coordination of the eight oxygen atoms at the interface between two tetrads.

The results with Li^+ , Na^+ and K^+ contrast those obtained with Rb^+ , NH_4^+ and Cs^+ , which show RMSD values about three times larger than the former with different varying degrees of structural distributions. As shown earlier, the hexadecamer \mathbf{mAGi}_{16} promoted by NH_4^+ shows slightly higher thermal stability than the one promoted by Na^+ , which correlates with reports from the literature in which ammonium cations have proven useful in studies of cation dynamics in OGQs and SGQs by NMR (25) and MS (26). Moreover, while $\mathbf{mAGi}_{16}\cdot 3NH_4^+$ gives a narrow structural distribution, the resulting RMSD is three times higher (~ 12 Å) than that of Na^+ . This seemingly conflicting result is likely a consequence of the specific coordination of the ammonium cations in which the resulting H-bonds impose relative orientations between the G-tetrads that deviate from those imposed by the spherical alkali cations.

As mentioned earlier, the two largest alkali cations evaluated (Rb^+ and Cs^+) induced significant structural distortions that are evident in the molecular models (Figure 7) and as reflected by the large RMSD values. The hexadecamer $\mathbf{mAGi}_{16}\cdot 3Rb^+$ showed a broader structural distribution than $\mathbf{mAGi}_{16}\cdot 3Cs^+$, while the latter resulted in the highest average RMSD value (Figure 6). A visual inspection of both hexadecamers (Figure 7) reveals significant structural distortions such as an offset of the tetrads and a displacement of the subunits relative to the initial central axis (Figure 7). These structural distortions result in diminished non-covalent interactions (e.g. $\pi-\pi$), and the loss of a cation from the inner/outer tetrad interface, all of which is consistent with the low fidelity and stability evident from the NMR studies (Figure 2). A

closer look at the models show that, in the case of structures (**mAGi**₆) containing Li⁺, NH₄⁺, Rb⁺ and Cs⁺, one cation from the outer tetrad is expelled from the channel.

Conclusion

This work illustrates how the cation size, charge and electron density provide a suitable strategy to modulate the self-assembly of **mAGi** into SGQs of different molecularities and stabilities. Monovalent cations with a size in the range of 1.18–1.66 Å (K⁺, Na⁺, Rb⁺ and NH₄⁺) promote the formation of the corresponding hexadecamer while, for smaller (Li⁺) or larger (Cs⁺) cations, the equilibrium is shifted towards an octamer or unidentified aggregates, respectively. Divalent cations within that size range also promote the formation of the corresponding octamers that are thermally more stable (at least for Sr²⁺ and Ba²⁺) than even the K⁺-promoted hexadecamer. We expect these findings to lead to the design and construction of multifunctional supramolecular systems with tuneable structure and dynamics for a wide variety of applications.

Experimental

Detailed experimental conditions, additional NMR spectra, molecular models, and MDS data are included in the Supplementary Information available online.

Funding

The authors thank the NIH-SCoRE [grant number 5SC1GM093994] for financial support and for graduate fellowships: NIH-RISE (2R25GM61151) (M.M.H., M.G.A.), the Alfred P. Sloan Foundation (MMH), PRIDCO (M.M.H.) and NSF-EPSCoR (EPS0223152) (M.G.A.).

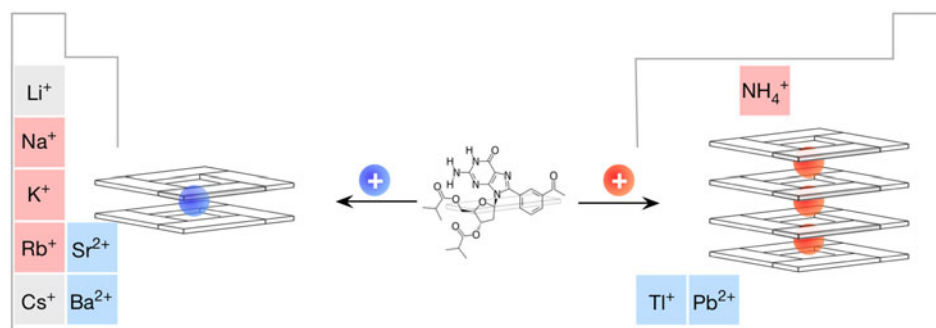
Note

1. See supplementary information for methodological details.

References

- (1) Lena, S.; Masiero, S.; Pieraccini, S.; Spada, G.P. *Chem. Eur. J.* **2009**, *15*, 7792–7806.
- (2) (a) Davis, J.T. *Angew. Chem. Int. Ed.* **2004**, *43*, 668–698; (b) Davis, J.T.; Spada, G.P. *Chem. Soc. Rev.* **2007**, *36*, 296–313.
- (3) (a) Gubala, V.; Betancourt, J.E.; Rivera, J.M. *Org. Lett.* **2004**, *6*, 4735–4738; (b) Rivera, L.R.; Betancourt, J.E.; Rivera, J.M. *Langmuir* **2011**, *27*, 1409–1414; (c) Rivera-Sánchez, M.D.C.; Andújar-de-Sanctis, I.; García-Arriaga, M.; Gubala, V.; Hobley, G.; Rivera, J.M. *J. Am. Chem. Soc.* **2009**, *131*, 10403–10405.
- (4) (a) González-Rodríguez, D.; van Dongen, J.L.J.; Lutz, M.; Spek, A.L.; Schenning, A.P.H.J.; Meijer, E.W. *Nature Chem.* **2009**, *1*, 151–155; (b) Shi, X.; Fettinger, J.C.; Davis, J.T. *Angew. Chem. Int. Ed.* **2001**, *40*, 2827–2831; (c) Shi, X.; Mullaugh, K.M.; Fettinger, J.C.; Jiang, Y.; Hofstadler, S.A.; Davis, J.T. *J. Am. Chem. Soc.* **2003**, *125*, 10830–10841.
- (5) (a) Betancourt, J.E.; Martín-Hidalgo, M.; Gubala, V.; Rivera, J.M. *J. Am. Chem. Soc.* **2009**, *131*, 3186–3188; (b) Pieraccini, S.; Bonacchi, S.; Lena, S.; Masiero, S.; Montalti, M.; Zaccheroni, N.; Spada, G.P. *Org. Biomol. Chem.* **2010**, *8*, 774–781.
- (6) García-Arriaga, M.; Hobley, G.; Rivera, J.M. *J. Am. Chem. Soc.* **2008**, *130*, 10492–10493.
- (7) Martín-Hidalgo, M.; Rivera, J.M. *Chem. Commun.* **2011**, *47*, 12485–12487.
- (8) Plavec, J. In *Metal complex–DNA interactions*; Hadjiliadis, N.D., Sletten, E., Eds.; John Wiley & Sons Ltd: Chichester, 2009; pp 55–94.
- (9) Todd, E.M.; Quinn, J.R.; Park, T.; Zimmerman, S.C. *Isr. J. Chem.* **2005**, *45*, 381–389.
- (10) Wong, A.; Wu, G. *J. Am. Chem. Soc.* **2003**, *125*, 13895–13905.
- (11) (a) Kotch, F.; Fettinger, J.; Davis, J. *Org. Lett.* **2000**, *2*, 3277–3280; (b) Kwan, I.C.M.; She, Y.-M.; Wu, G. *Can. J. Chem.* **2011**, *89*, 835–844; (c) van Leeuwen, F.W.B.; Verboom, W.; Shi, X.; Davis, J.T.; Reinhoudt, D.N. *J. Am. Chem. Soc.* **2004**, *126*, 16575–16581.
- (12) (a) Kwan, I.C.M.; She, Y.-M.; Wu, G. *Chem. Commun.* **2007**, 4286–4288; (b) Shinoda, S.; Noguchi, T.; Ikeda, M.; Habata, Y.; Tsukube, H. *J. Incl. Phenom. Macrocycl. Chem.* **2011**, *71*, 523–527.
- (13) (a) Gubala, V.; De Jesus, D.; Rivera, J.M. *Tetrahedron Lett.* **2006**, *47*, 1413–1416; (b) Martín-Hidalgo, M.; Camacho-Soto, K.; Gubala, V.; Rivera, J.M. *Supramol. Chem.* **2010**, *22*, 862–869; (c) van Leeuwen, F.W.B.; Davis, J.T.; Verboom, W.; Reinhoudt, D.N. *Inorg. Chim. Acta* **2006**, *359*, 1779–1785.
- (14) Shannon, R.D. *Acta Crystallogr Sect. A* **1976**, *32*, 751–767.
- (15) Sponer, J.; Spacková, N.A.A. *Methods* **2007**, *43*, 278–290.
- (16) (a) Davis, J.; Tirumala, S.; Marlow, A. *J. Am. Chem. Soc.* **1997**, *119*, 5271–5272; (b) Shi, X.; Fettinger, J.; Cai, M.; Davis, J. *Angew. Chem. Int. Ed.* **2000**, *39*, 3124–3127; (c) Nikan, M.; Sherman, J.C. *J. Org. Chem.* **2009**, *74*, 5211–5218.
- (17) (a) Neidle, S.; Parkinson, G.N. *Biochimie* **2008**, *90*, 1184–1196; (b) Lee, M.P.H.; Parkinson, G.N.; Hazel, P.; Neidle, S. *J. Am. Chem. Soc.* **2007**, *129*, 10106–10107; (c) Gill, M.L.; Strobel, S.A.; Loria, J.P. *Nucleic Acids Res.* **2006**, *34*, 4506–4514.
- (18) (a) Ma, L.; Iezzi, M.; Kaucher, M.S.; Lam, Y.-F.; Davis, J.T. *J. Am. Chem. Soc.* **2006**, *128*, 15269–15277; (b) Hud, N.V.; Plavec, J. In *Quadruplex Nucleic Acids*. Royal Society of Chemistry: Cambridge, **2006**, pp 100–130.
- (19) (a) Liu, W.; Zhu, H.; Zheng, B.; Cheng, S.; Fu, Y.; Li, W.; Lau, T.C.; Liang, H. *Nucleic Acids Res.* **2012**, *40*, 4229–4236; (b) Liu, W.; Zheng, B.; Cheng, S.; Fu, Y.; Li, W.; Lau, T.-C.; Liang, H. *Soft Matter* **2012**, *8*, 7017–7023; (c) Majhi, P.R.; Shafer, R.H. *Biopolymers* **2006**, *82*, 558–569; (d) Smirnov, I.V.; Kotch, F.W.; Pickering, I.J.; Davis, J.T.; Shafer, R.H. *Biochemistry* **2002**, *41*, 12133–12139; (e) Smirnov, I.; Shafer, R.H. *J. Mol. Biol.* **2000**, *296*, 1–5.
- (20) (a) Yang, C.; Liu, L.; Zeng, T.; Yang, D.; Yao, Z.; Zhao, Y.; Wu, H.-C. *Anal. Chem.* **2013**, *85*, 7302–7307; (b) Li, X.; Wang, G.; Ding, X.; Chen, Y.; Gou, Y.; Lu, Y. *Phys. Chem. Chem. Phys.* **2013**, *15*, 12800–12804; (c) Li, T.; Dong, S.; Wang, E. *J. Am. Chem. Soc.* **2010**, *132*, 13156–13157; (d) Li, T.; Wang, E.; Dong, S. *J. Am. Chem. Soc.* **2009**, *131*,

- 15082–15083; (e) Elbaz, J.; Shlyahovsky, B.; Willner, I. *Chem. Commun.* **2008**, 1569–1571.
- (21) Fadrná, E.; Spacková, N.a.a.; Stefl, R.; Koca, J.; Cheatham, T.E.; Sponer, J. *Biophys. J.* **2004**, *87*, 227–242.
- (22) Reshetnikov, R.V.; Sponer, J.; Rassokhina, O.I.; Kopylov, A.M.; Tsvetkov, P.O.; Makarov, A.A.; Golovin, A.V. *Nucleic Acids Res.* **2011**, *39*, 9789–9802.
- (23) Akhshi, P.; Mosey, N.J.; Wu, G. *Angew. Chem. Int. Ed.* **2012**, *51*, 2850–2854.
- (24) Bowman, J.C.; Lenz, T.K.; Hud, N.V.; Williams, L.D. *Curr. Opin. Struct. Biol.* **2012**, *22*, 262–272.
- (25) (a) Sket, P.; Virgilio, A.; Esposito, V.; Galeone, A.; Plavec, J. *Nucleic Acids Res.* **2012**, *40*, 11047–11057; (b) Zavasnik, J.; Podbevsek, P.; Plavec, J. *Biochemistry* **2011**, *50*, 4155–4161; (c) Trajkovski, M.; Sket, P.; Plavec, J. *Org. Biomol. Chem.* **2009**, *7*, 4677–4684; (d) Podbevsek, P.; Sket, P.; Plavec, J. *J. Am. Chem. Soc.* **2008**, *130*, 14287–14293; (e) Sket, P.; Plavec, J. *J. Am. Chem. Soc.* **2007**, *129*, 8794–8800; (f) Podbevsek, P.; Sket, P.; Plavec, J. *Nucleos. Nucleot. Nucl.* **2007**, *26*, 1547–1551; (g) Podbevsek, P.; Hud, N.V.; Plavec, J. *Nucleic Acids Res.* **2007**, *35*, 2554–2563; (h) Hud, N.V.; Schultze, P.; Sklenár, V.; Feigon, J. *J. Mol. Biol.* **1999**, *285*, 233–243.
- (26) (a) Rosu, F.; Gabelica, V.; Poncelet, H.; De Pauw, E. *Nucleic Acids Res.* **2010**, *38*, 5217–5225; (b) Amato, J.; Oliviero, G.; De Pauw, E.; Gabelica, V. *Biopolymers* **2009**, *91*, 244–255; (c) Mazzitelli, C.L.; Wang, J.; Smith, S.I.; Brodbelt, J.S. *J. Am. Soc. Mass Spectrom.* **2007**, *18*, 1760–1773; (d) Guo, X.; Liu, S.; Yu, Z. *J. Am. Soc. Mass Spectrom.* **2007**, *18*, 1467–1476.



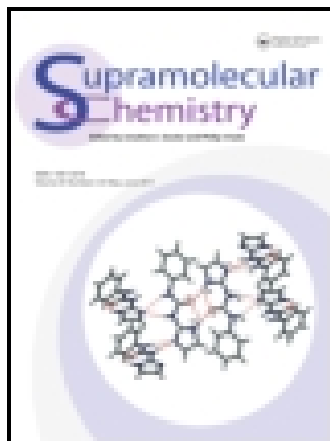
Mariana Martín-Hidalgo, Marilyn García-Arriaga, Fernando González and José M. Rivera

Tuning supramolecular G-quadruplexes with mono- and divalent cations

1–8

Publisher: Taylor & Francis

Informa Ltd Registered in England and Wales Registered Number: 1072954 Registered office: Mortimer House, 37-41 Mortimer Street, London W1T 3JH, UK



Supramolecular Chemistry

Publication details, including instructions for authors and subscription information:

<http://www.tandfonline.com/loi/gsch20>

Tuning supramolecular G-quadruplexes with mono- and divalent cations

Mariana Martín-Hidalgo^a, Marilyn García-Arriaga^a, Fernando González^a & José M. Rivera^a

^a Department of Chemistry, University of Puerto Rico, Río Piedras Campus, Río Piedras 00931, Puerto Rico

Published online: 25 Jun 2014.



[Click for updates](#)

To cite this article: Mariana Martín-Hidalgo, Marilyn García-Arriaga, Fernando González & José M. Rivera (2014): Tuning supramolecular G-quadruplexes with mono- and divalent cations, *Supramolecular Chemistry*, DOI: [10.1080/10610278.2014.924626](https://doi.org/10.1080/10610278.2014.924626)

To link to this article: <http://dx.doi.org/10.1080/10610278.2014.924626>

PLEASE SCROLL DOWN FOR ARTICLE

Taylor & Francis makes every effort to ensure the accuracy of all the information (the "Content") contained in the publications on our platform. However, Taylor & Francis, our agents, and our licensors make no representations or warranties whatsoever as to the accuracy, completeness, or suitability for any purpose of the Content. Any opinions and views expressed in this publication are the opinions and views of the authors, and are not the views of or endorsed by Taylor & Francis. The accuracy of the Content should not be relied upon and should be independently verified with primary sources of information. Taylor and Francis shall not be liable for any losses, actions, claims, proceedings, demands, costs, expenses, damages, and other liabilities whatsoever or howsoever caused arising directly or indirectly in connection with, in relation to or arising out of the use of the Content.

This article may be used for research, teaching, and private study purposes. Any substantial or systematic reproduction, redistribution, reselling, loan, sub-licensing, systematic supply, or distribution in any form to anyone is expressly forbidden. Terms & Conditions of access and use can be found at <http://www.tandfonline.com/page/terms-and-conditions>